Barriers about Double Carbon-Nitrogen Bond in Imine Derivatives (Aldimines, Oximes, Hydrazones, Azines)*

Fernando Blanco, Ibon Alkorta, ** **and José Elguero**

Instituto de Química Médica, C.S.I.C. Juan de la Cierva 3, E-28006 Madrid, Spain

Abstract. The paper presents the results referring to the inversion mechanism of imines and their derivatives (hydrazones, oximes, azines). The calculated barriers [B3LYP/6-311++G(d,p) and G3B3)] are in good agreement with the scarce existing data. The transition states correspond in all cases to a pure nitrogen inversion except in the case of azines where they have some rotation character. The electron properties of the minima and the transition states have been characterized, allowing explanation of the geometrical changes observed in the process.

Keywords: imines, hydrazones, oximes, azines, inversion mechanism, DFT calculations, G3B3 calculations

INTRODUCTION

The *E/Z* isomerism of imines is a classical problem of stereochemistry[1] that has been recently summarized by Lehn[2] in his Figure 1 (adapted from Ref. 2) in an attempt to use imines as unidirectional photodriven molecular motors.

What is of fundamental importance in Figure 1 is that the isomerization takes place by inversion in the ground state and by rotation in the excited state (this is the base of photodriven motors). We have decided to examine again this problem limiting ourselves to the ground state, that is, to the inversion mechanism, but extending considerably the nature of R because we have found some indications that in azines (R = N=CR'R") the mechanism is a mixed rotation/inversion one.[3] Note that some authors call the inversion "in-plane rotation" and the rotation, "out-of-plane rotation".

The compounds studied are represented in Figure 2. They cover imines, **1−4**, hydrazones, **5** and **6**, oximes **7**, N−N derivatives, **8−10**, *N*-fluoroimine **11**, and four azines **12−15**.

METHODS

The calculations have been carried out at the B3LYP/6-311++G(d,p) level[4–7] with the Gaussian-03 package.[8] Harmonic frequencies were calculated to verify that the obtained structures correspond to minima (all real frequencies) or to transition states (one imaginary frequency).[9] Additionally, G3B3 calculations were performed to obtain accurate values of the free energy of the processes.[10]

The Natural Bond Orbital (NBO) methodology[11] provides a Lewis like representation of the molecular orbital and allows to analyze the interaction between occupied and unoccupied molecular orbitals. The shape of the orbitals has been represented with the NBOview software.
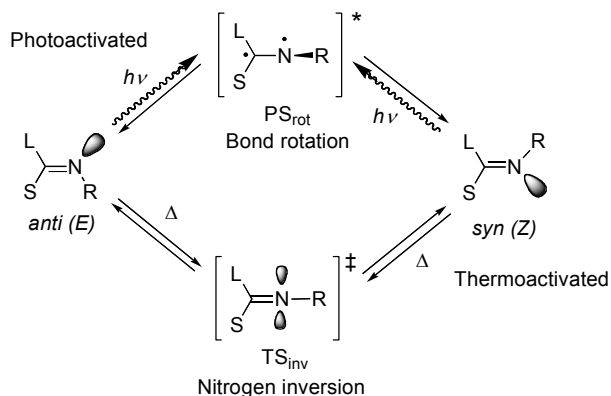
Figure 1. Schematic representation of the rotation and inversion processes in imines.

---

* Dedicated to Professor Zvonimir Maksić on the occasion of his 70th birthday.
** Author to whom correspondence should be addressed. (E-mail: ibon@iqm.csic.es)
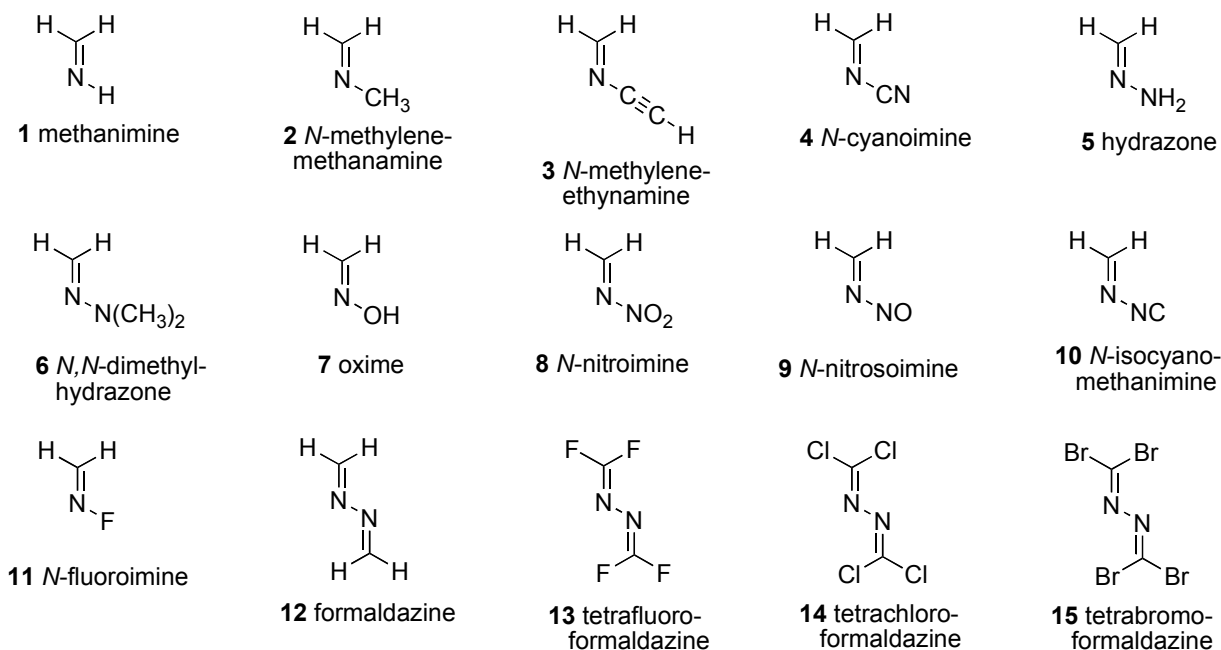
Figure 2. The 15 studied compounds.

The electron density of the systems has been analyzed within the Atoms In Molecules (AIM)[12] methodology with the AIMPAC and MORPHY packages.[13,14] The topological analysis of the electron density reveals the presence of saddle points, characterized by two negative curvatures and a positive one. These points are known as bond critical points and it properties have shown to characterized those of the bond. The atomic properties have been obtained by integration within the atomic basins. The integration conditions have been changed in order to obtain integrated Laplacian for each atomic basin smaller than 1×10^{-3} in absolute value since previous studies have shown that the errors in the energy and charge in these conditions are very small.[15]

The electron localization function (ELF)[16] has been calculated using the TOPMOD package.[17] This function ranges between 0 and 1, becoming large in regions of space where electron pairs are localized, either as bonding or lone pairs. A conventional of ELF = 0.7 has been adopted for the representation in the present article.

RESULTS AND DISCUSSION

We have reported the results obtained in Tables 1 (energies in kJ mol^{-1})[11–20] and 2 (geometries in Å, º) for the minima and TSs of compounds **1**–**8**. Since all compounds derive from formaldehyde, the *E* and *Z* isomers are identical.

The G3B3 barriers are systematically higher than B3LYP/6-311++G(d,p) ones but both are highly corre-

lated: G3B3 = (18.8±2.3) + (0.984±0.02)*B3LYP, *n* = 14, R^2 = 0.997. The G3B3 predicted value of **15** is 83.3 kJ mol^{-1}.

In the case of simple imines like **1** the rotation mechanism through an excited state (Figure 1) has been studied many times,[28–34] but it lies outside the scope of the present paper.

The calculations reproduce adequately the cases of compounds **1**, **2** and **4**. For compound **6**, the replacement of two benzyl groups (experiment) by two methyl groups (calculations) is not a good approximation. Finally, the calculated high barriers of oxime **7** and *N*-fluoroimine **11** explain why these compounds do not isomerize in the gas phase. The very large increase in the barrier on going from **1** (N−H) to **11** (N−F) is comparable with the experimental result found in the nitrogen inversion of saturated heterocycles.[35]

The calculated values by other authors for the nitrogen inversion (four systems) and our results agree very well even if their methods differ from one author to the other.

The calculated barriers show some regularities with Pauling electronegativities[36] with the exception of the *N*-nitrosimino derivative **9** which has the lowest barrier of all compounds of Table 1.

The geometries of the minima and TS structures have been gathered in Table 2 and Figures 4 and 5. Note that all the TS (Figure 5) correspond to "perfect" bond inversion structures except the azines **12**–**15** that show mixed rotation-inversion TSs. On going from the

Table 1. Barriers (ΔG in kJ mol^{-1}) corresponding to compounds **1–15**

Comp.	Symm. of the min	Symm. of the TS	Calculated barrier (ΔG / kJ mol^{-1})		Lit. calc. barrier (ΔG / kJ mol^{-1})	Lit. exp. Barrier (ΔG / kJ mol^{-1})
			B3LYP/ 6-311++G(d,p)	G3B3		
1	C_s	C_{2v}	107.8	116.0	117.2 CASPT2/cc-pVTZ[a] 211.2, 6-31G* (rot.)[b] 195.4, CID/6-31G* (rot.)[b] 135.9, 6-31G* (inv.)[b]	104-113 (*C*-methyl derivatives)[c]
2	C_s	C_s	109.4	126.0	-----	104-113 (*C*-methyl derivatives)[c]
3	C_s	C_{2v}	56.9	72.6	-----	No experimental data.
4	C_s	C_{2v}	64.0	76.8	-----	79.1 (*C*-methyl derivatives)[d]
5	C_1	C_s	135.6	156.1	137.6, 6-31G**[e] 128.4 (triplet)[e]	No experimental data.
6	C_1	C_s	128.8	149.6	-----	90.4 (*N,N*-dibenzyl, *C*-methyl derivatives)[f]
7	C_s	C_s	231.9	246.7	246.0, 6-31G**[e] 140.6 (triplet)[e] 237.7[g] B3LYP/6-311++G**	No isomerization in the gas phase[h],[i]
8	C_1	C_s	124.3	141.3	-----	No experimental data.
9	C_s	C_s	45.1	62.4	-----	No experimental data.
10	C_s	C_{2v}	140.7	159.0	-----	No experimental data.
11	C_s	C_{2v}	307.7	319.7	333.0, 6-31G**[e] The triplet dissociates[e]	No isomerization in the gas phase[j]
12	C_{2h}	C_s	92.7	117.6	96.5[k]	No experimental data.
13	C_{2h}	C_s	88.5	105.7	91.8[k]	No experimental data.
14	C_2	C_s	72.8	93.2	74.2[k]	No experimental data.
15	C_2	C_s	65.5	---	66.7[k]	No experimental data.

[a] From ref. 18. [b] From ref. 19. [c] From ref. 20. [d] From ref. 21. [e] From ref. 22. [f] From ref. 23. [g] From ref. 24. [h] From ref. 25. [i] From ref. 26. [j] From ref. 27. [k] These values correspond to SCF energies.[3]

Table 2. Geometries corresponding to minima and TSs of compounds **1–15** at the B3LYP/6-311++G(d,p) level

Compd.	CN (min) Å	CN (TS) Å	diff. Å	NX (min) Å	NX (TS) Å	diff. Å
1	1.267	1.236	−0.031	1.023	0.990	−0.033
2	1.263	1.237	−0.026	1.452	1.399	−0.054
3	1.276	1.251	−0.025	1.335	1.269	−0.066
4	1.276	1.250	−0.025	1.338	1.270	−0.069
5	1.274	1.253	−0.020	1.367	1.281	−0.086
6	1.282	1.258	−0.024	1.354	1.282	−0.072
7	1.268	1.244	−0.025	1.402	1.315	−0.087
8	1.267	1.245	−0.022	1.487	1.315	−0.172
9	1.273	1.258	−0.014	1.488	1.265	−0.223
10	1.276	1.247	−0.029	1.343	1.247	−0.095
11	1.263	1.241	−0.023	1.422	1.320	−0.102
12	1.272	1.251	−0.021	1.416	1.249	−0.168
13	1.255	1.254	−0.001	1.396	1.316	−0.081
14	1.264	1.270	0.007	1.373	1.288	−0.085
15	1.260	1.271	0.010	1.369	1.285	−0.085

Table 3. Properties of the minima and transition states as defined by bond properties

Compd.	bond order NBO C=N		ellipticity AIM C=N		bond order NBO N−X		ellipticity AIM N−X	
	min	TS	min	TS	min	TS	min	TS
1	2.034	2.046	0.192	0.120	0.868	0.806	0.021	0.065
2	1.968	1.973	0.217	0.155	1.032	1.051	0.012	0.015
3	1.818	1.777	0.174	0.148	1.204	1.332	0.025	0.017
4	1.826	1.796	0.139	0.103	1.184	1.306	0.006	0.059
5	1.870	1.811	0.309	0.350	1.148	1.251	0.083	0.045
6	1.811	1.796	0.296	0.339	1.166	1.232	0.121	0.065
7	1.931	1.926	0.260	0.264	1.029	1.123	0.027	0.080
8	1.938	1.890	0.139	0.148	0.885	1.148	0.075	0.294
9	1.889	1.783	0.118	0.215	0.998	1.505	0.005	0.153
10	1.861	1.824	0.189	0.161	1.103	1.237	0.022	0.134
11	1.989	1.987	0.227	0.203	0.898	1.022	0.038	0.209
12	1.887	1.808	0.187	0.277	1.083	1.403	0.015	0.074
13	1.769	1.742	0.504	0.693	1.065	1.142	0.009	0.055
14	1.755	1.672	0.395	0.573	1.079	1.208	0.009	0.057
15	1.782	1.680	0.368	0.520	1.076	1.216	0.008	0.054

minimum to the TS, the C=N bond contracts (exceptions **14** and **15**) and the N−X bond also diminishes (no exceptions).

We have characterized the C=N and N−X bonds by means of three parameters: the bond lengths (Å, Table 2) as well as the NBO bond orders and the AIM ellipticities at the electron density bond critical point (bcp) (Table 3).
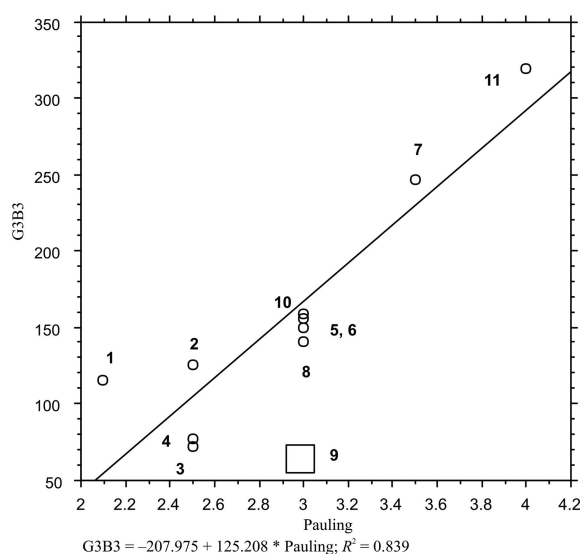
Figure 3. G3B3 barrier *vs.* the electronegativity of the atom attached to the N2.

The three criteria (bond distance, bond order and ellipticity) are related in some cases but the most interesting correlations are those relating the TS and the minima. To obtain significant correlations the three compounds bearing substituents on the iminic carbon atom (**13**, **14** and **15**) must be removed.

For the remaining 12 compounds, the R^2 values are: C=N bond length, 0.676, C=N bond order, 0.885 (Figure 3 left), C=N ellipticity, 0.563; N−X bond length, 0.798 (Figure 3 right), N−X bond order, 0.364, N−X ellipticity, 0.028. Taking into account that in Figure 6 right, the correlation is acceptable thanks to the N−H bond of compound **1**, the conclusion is that the variations in the N−X properties between the minimum and the TS cannot be used to characterize these compounds.

Another way to compare minima and TSs is to calculate the differences between the three parameters of the C=N bond (Tables 2 and 4) for compounds **1** to **12**.

In all cases the C=N bond length is longer in the minimum than in the TS; the bond order (as measured by NBO) is greater in the minimum than in the TS (larger variation for **9**) except in the imines **1** and **2**. The variations in ellipticity depends on the nature of the X atom: for X = C (**1**, **2**, **3** and **4**) the ellipticity decreases while for X = N or O it increases with the exception of the isonitrile **10**.
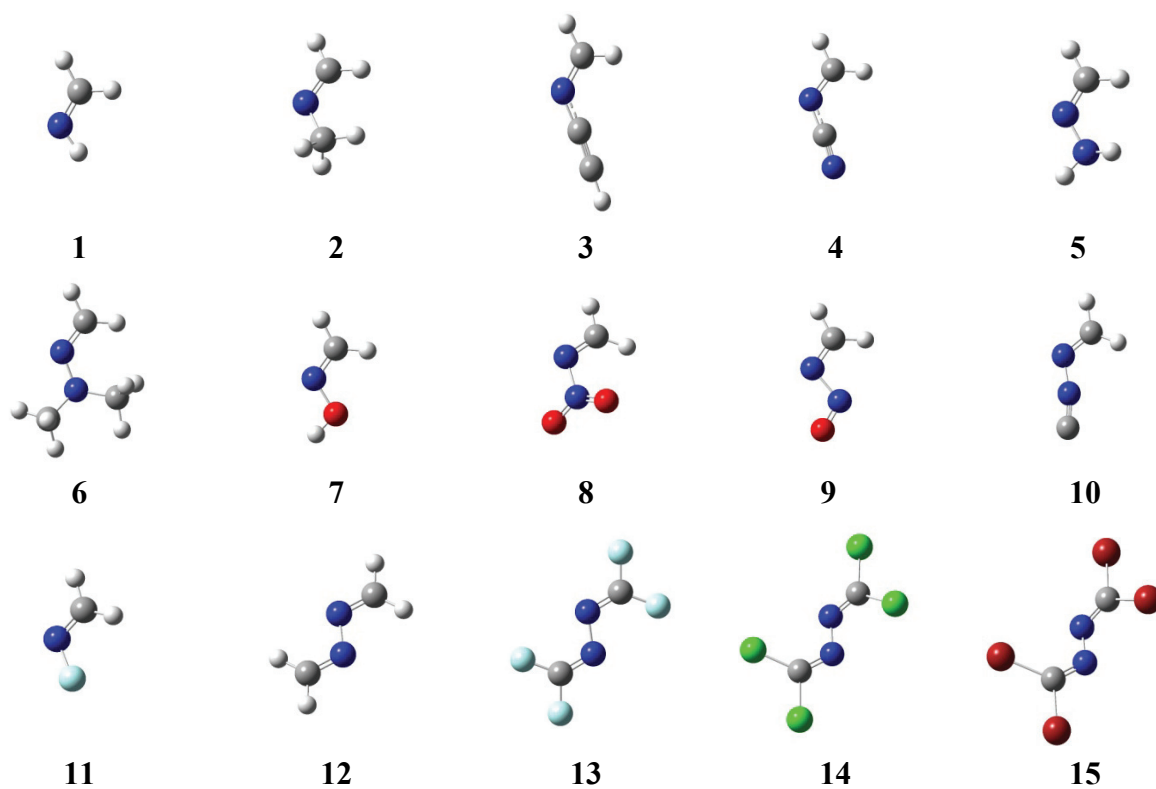
Figure 4. Drawing of the geometries of the minima.
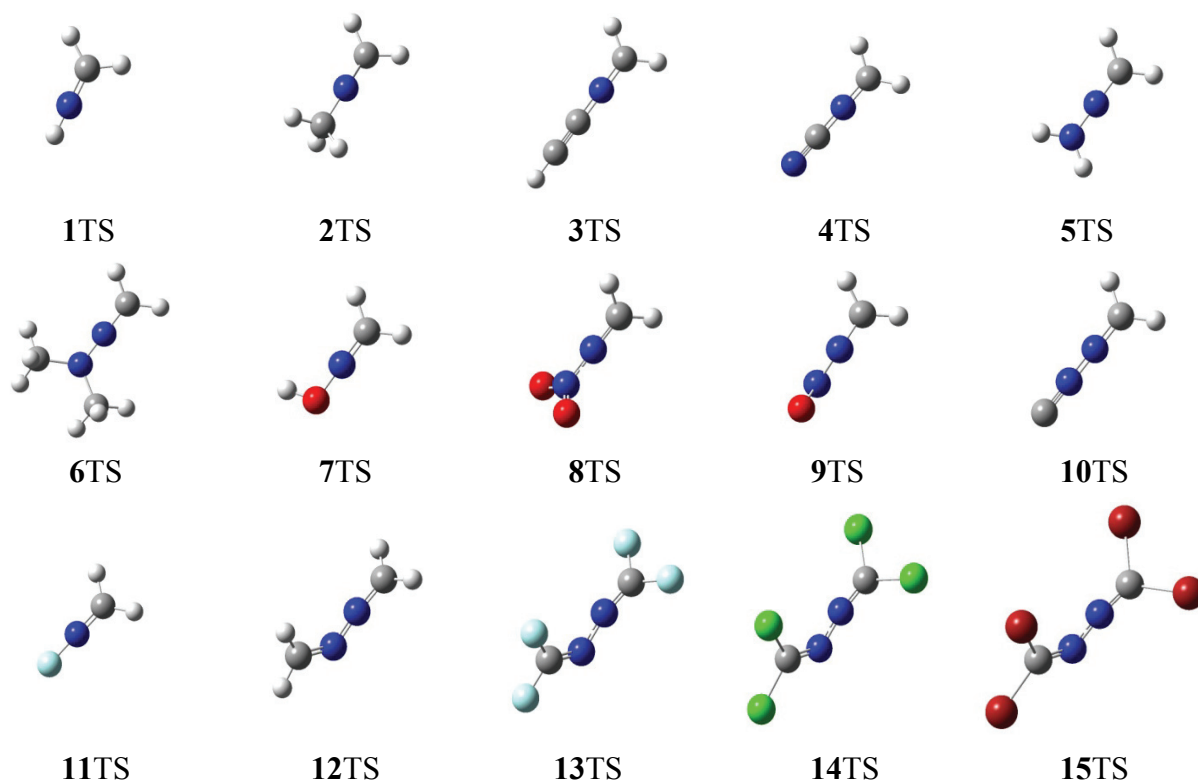
Figure 5. Drawing of the geometries of the TS.
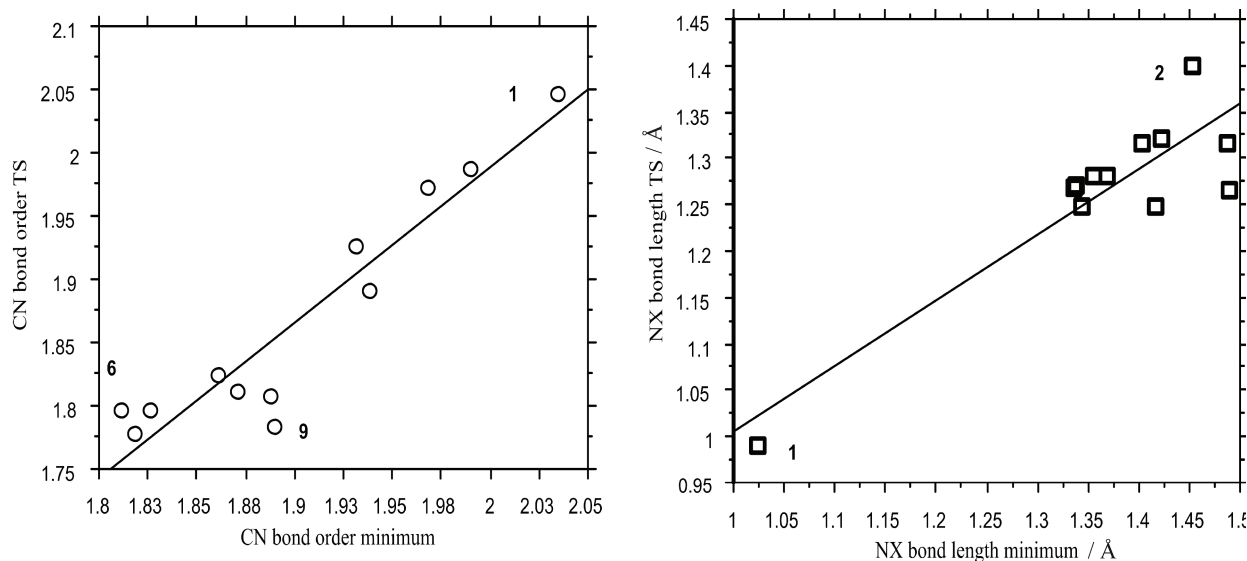
Figure 6. Comparison of the best-correlated properties of the TS and minima. Left: CN bond order of the TS = −(0.47±0.27) + (1.23±0.14) * CN bond order of the minima, $n = 12$, $R^2 = 0.89$. Right: NX bond length of the TS = (0.30±0.16) Å + (0.71±0.11) Å * NX bond length of the minima, $n = 12$, $R^2 = 0.80$.

The analysis of the electronic properties of the minima and TS structures shows that while in the minima the lone pair associated to the nitrogen atom presents a sp^2 character, in the TS they have a p character with two identical lobules at each side of the nitrogen atom (Scheme 1). This conclusion can be reached by analyzing the minima in the electrostatic potential maps, shape of the ELF function, location of the minima in the Laplacian of the electron density or the NBO orbitals associated to the lone pair (Figure 7). In all the analysis, it can be seen that the lone pair in the TS is located in the plane of the molecule and orthogonal to the π-orbital of the C=N bond.

In addition, the disposition and p character of the nitrogen lone pair in the TS indicate that this orbital partially formed a triple bond for the C−N bond and a double bond for the N−X one. Thus, the contribution of

Table 4. Differences between TS and minimum (Diff. = $X_{TS} − X_{min}$) of the C=N bond

Compd.	Bond order	Ellipticity
1	0.013	−0.072
2	0.004	−0.062
3	−0.041	−0.025
4	−0.031	−0.036
5	−0.059	0.041
6	−0.015	0.043
7	−0.005	0.004
8	−0.048	0.010
9	−0.106	0.097
10	−0.037	−0.028
11	−0.002	−0.024
12	−0.080	0.090

the nitrogen atom to the σ bond, based on the NBO analysis, is approximately sp^2 in the minima an sp in the TS (Table 5). This change of hybridization is responsible that both CN and NX bond shortened in the TS up to 0.03 and 0.22 Å, respectively. The molecules **13−15** that are the only cases that present atoms other than hydrogens bonded to the C1 do not follow the tendencies above mentioned.

Among other electronic effects observed in the NBO analysis corresponds to the charge transfer from the lone pair or the C−N bond and the antibonding orbital of those X groups with multiple bonds (Table 6). In addition, a back donation is observed between the multiple bonds of the X groups and the CN antibonding orbital. It is significant that all the structures with TS barriers bellow 100 kJ mol^{-1} are among those that present large values of the interaction between the lone pair with the antibonding multiple bond of X in the TS structures (between 67 to 477 kJ mol^{-1}).

In addition an important interaction of the nitrogen lone pair with the CH antibonding orbital (between 59 and 96 kJ mol^{-1}) is observed in the TS structures which produces a significant elongation of these bonds (up to 0.025 Å). In the minima structures, this orbital interaction is only between the lone pair and the CH antibonding orbital in trans disposition (between 25 and 50 kJ
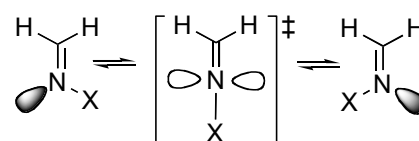
Scheme 1.
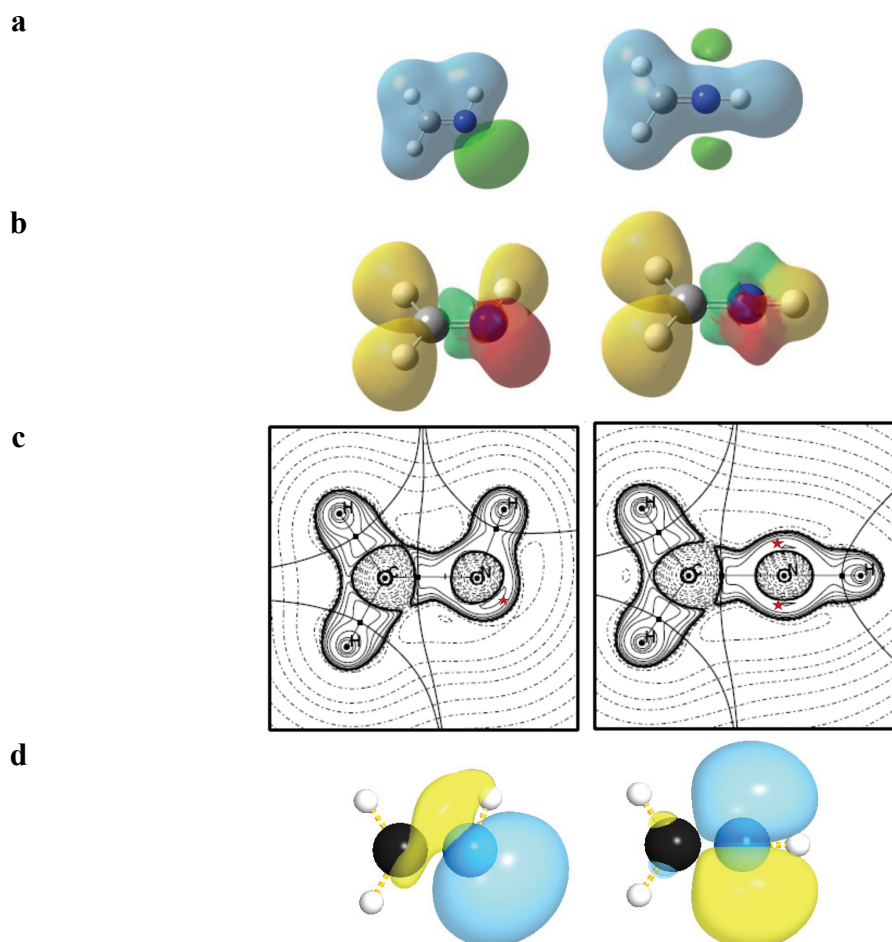
Figure 7. Electronic properties of **1** minimum (left) and TS (right): a) Molecular Electrostatic Potential at ± 0.03 a.u. (Green and blue regions represent negative and positive values, respectively); b) Electron localization function at a value of 0.7 (Yellow, green and red represent valence protonated disynaptic, valence disynaptic and valence (lone pair), respectively); c) Laplacian of the electron density, the minimum location in indicated with a star. In continuous lines, negative regions and in dashed lines, positive ones; d) Isosurface of the NBO lone pair (Yellow and blue represent positive and negative values).

mol^{-1}) but its value is smaller than the one observed in the TS case. These effect, which results in a elongation of the CH bond, can be observed in the disposition of the lone pair orbital represented in Figure 7d, where the cloud of the lone pair cover part of the C−H bonds in the minima and TS structures.

The topological analysis of the electron density shows interesting features in the distribution of the electron density values at the bond critical point (bcp) *vs*. the distance in the CN bond (Figure 8). In general, exponential relationships[37−41] have been described for the comparison of this property in a variety of bonds. However, in this case, the data are clustered based on the minimum or TS structures showing two independent correlations. A similar tendency is observed for the Laplacian at the BCP being the values of some of the TS structures positive. All these results indicate that a clear depletion of charge is observed in the CN bcp in

the TS. Thus, the region where the bcp is located, much closer to the carbon atom than to the nitrogen one, is not populated effectively since the lone pair is centered on the nitrogen atom.

In all the structures, minima and TS, the corresponding minima of the Laplacian due to the lone pair of the nitrogen have been located (an example is given in Figure 7c). The values are larger, in absolute value, for the minima structures (−2.70 to −3.36 a.u.) than in the corresponding two minima found in the TS structures (−1.64 to −2.86 a.u.). These results are in agreement with the expected larger concentration of charge in the minima than in the splitted lone pair of the TS. A correlation (Figure 9) can be found between the value of the Laplacian minima and its corresponding distance to the nitrogen atom. Those cases with larger Laplacian are closer to the nitrogen atoms. A similar correlation has been described for a series of pyridine derivatives.[42]

Table 5. Atomic orbital contribution to the molecular orbital based on the NBO analysis

Compd.	σ C1N2 (min)		σ C1N2 (TS)		Lone pair (min)	Lone pair (TS)
	C	N	C	N	N2	N2
1	$sp^{1.68}$	$sp^{1.42}$	$sp^{1.73}$	$sp^{0.88}$	$sp^{1.57}$	p
2	$sp^{1.74}$	$sp^{1.45}$	$sp^{1.79}$	$sp^{0.91}$	$sp^{2.26}$	p
3	$sp^{1.81}$	$sp^{1.52}$	$sp^{1.88}$	$sp^{0.96}$	$sp^{2.74}$	p
4	$sp^{1.82}$	$sp^{1.49}$	$sp^{1.89}$	$sp^{0.92}$	$sp^{2.40}$	p
5	$sp^{2.66}$	$sp^{2.04}$	$sp^{2.07}$	$sp^{0.77}$	$sp^{2.00}$	p
6	$sp^{3.51}$	$sp^{2.80}$	$sp^{2.11}$	$sp^{0.81}$	$sp^{2.10}$	p
7	$sp^{1.87}$	$sp^{1.35}$	$sp^{2.01}$	$sp^{0.59}$	$sp^{1.36}$	p
8	$sp^{2.00}$	$sp^{1.60}$	$sp^{2.00}$	$sp^{0.69}$	$sp^{1.21}$	p
9	$sp^{1.82}$	$sp^{1.52}$	$sp^{2.25}$	$sp^{0.81}$	$sp^{1.23}$	p
10	$sp^{1.87}$	$sp^{1.49}$	$sp^{1.99}$	$sp^{0.73}$	$sp^{1.69}$	p
11	$sp^{1.87}$	$sp^{1.44}$	$sp^{2.05}$	$sp^{0.52}$	$sp^{1.03}$	p
12	$sp^{1.81}$	$sp^{1.46}$	$sp^{2.18}$	$sp^{0.84}$	$sp^{1.60}$	p
13	$sp^{1.25}$	$sp^{1.75}$	$sp^{1.30}$	$sp^{1.65}$	$sp^{1.49}$	$sp^{1.82}$
14	$sp^{1.54}$	$sp^{1.40}$	$sp^{1.60}$	$sp^{1.31}$	$sp^{1.92}$	$sp^{2.31}$
15	$sp^{1.57}$	$sp^{1.31}$	$sp^{0.63}$	$sp^{1.24}$	$sp^{2.09}$	$sp^{2.49}$

Table 6. Orbital interaction energies obtained within the NBO methodology (kJ mol^{-1})

Compd.	Lone pair (N2)→π* (X3−Y4)		π (CN)→π* (X3Y4)		π(X3Y4)→π* (CN)	
	Min	TS	Min	TS	Min	TS
1	---	---	---	---	---	---
2	---	---	---	---	---	---
3	15.36	76.22	20.36	19.06	16.84	31.15
4	13.65	73.63	21.55	20.99	11.73	22.41
5	---	--	---	---	---	---
6	---	---	---	---	---	---
7	---	---	---	---	---	---
8	2.37	114.03	8.73	4.92	2.35	1.06
9	1.15	128.08	16.96	7.00	3.84	1.11
10	6.55	53.27	12.30	12.50	15.37	32.69
11	---	---	---	---	---	---
12	---	83.56	12.00	3.95	12.00	2.82
13	---	16.41	10.75	---	10.75	---
14	4.38	26.69	8.54	---	8.54	---
15	6.81	27.78	7.04	---	7.04	---

The variation of the group energy and charge from the minimum to the TS calculated by integration within the atomic basins has been gathered in Table 7. The results show that in all the cases, the nitrogen atom is stabilized in the TS while the CH$_2$ and X groups are energetically desta-bilized, with the exception of the ΔE(X) of **9**. These ener-getic variations parallel to the variation of charge. Thus, the nitrogen atom gains charge in the TS with respect to the minimum, with the exception of **9**, while the CH$_2$ and X ones lost it. Finally, small variations in the total volume of the molecules are observed between the minimum and TS structures, being in most of the cases the TS structure smaller than the minimum which could favor the process in high-pressure environments.
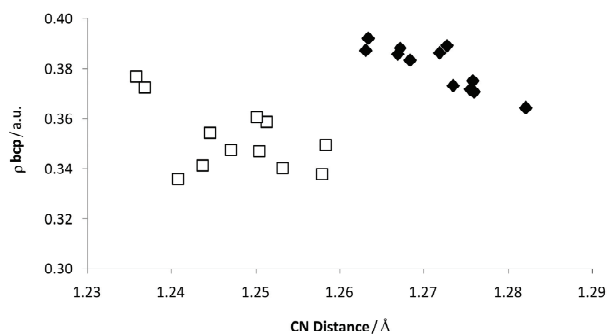
Figure 8. Electron density at the BCP, ρ_{BCP}, (a.u.) *vs.* the CN distance (Å). The white squares correspond to the TS structures and the black ones to the minima.
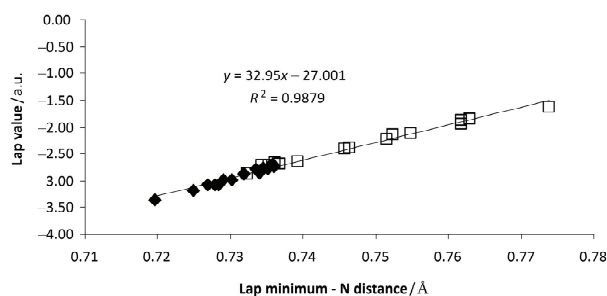
Figure 9. Value of the Laplacian (a.u.) minima associated with the lone pair *vs.* its distance to the nitrogen atom (Å). The white squares correspond to the TS structures and the black ones to the minima.

Table 7. Variation of the energy (kJ mol^{-1}), charge (*e*) and volume (a.u) obtained using the AIM method

Compd.	$\dfrac{\Delta E(CH_2)}{\text{kJ mol}^{-1}}$	$\dfrac{\Delta E(N)}{\text{kJ mol}^{-1}}$	$\dfrac{\Delta E(X)}{\text{kJ mol}^{-1}}$	$\dfrac{\Delta Q(CH_2)}{e}$	$\dfrac{\Delta Q(N)}{e}$	$\dfrac{\Delta Q(X)}{e}$	$\dfrac{\Delta\,\text{Vol.}}{\text{a.u.}}$
1	402.5	−535.6	247.4	0.121	−0.296	0.175	−0.7
2	386.3	−694.1	412.5	0.079	−0.263	0.162	−1.8
3	286.9	−755.1	433.2	0.062	−0.255	0.181	−0.6
4	290.4	−801.5	433.6	0.073	−0.293	0.181	−1.3
5	355.5	−501.0	288.0	0.023	−0.142	0.111	−2.3
6	387.9	−531.6	389.0	0.048	−0.157	0.151	8.7
7	438.5	−444.3	282.8	0.012	−0.128	0.144	−1.6
8	381.2	−524.5	190.3	0.078	−0.085	0.056	1.8
9	278.6	−418.3	−42.7	0.025	0.028	0.001	−10.2
10	397.9	−565.6	381.6	0.061	−0.151	0.178	1.0
11	485.1	−331.6	159.0	0.010	−0.134	0.123	−1.4
12	343.1	−510.5	301.5	0.004	−0.021	0.217	−3.1

CONCLUSION

We have obtained a comprehensive picture of the effect of *N*-substituents on the imines derived from formaldehyde. Except in the case of azines (F, Cl, Br), the effect of C-substituents has not been studied. More examples with different N- and C-substituents and more experimental determinations are necessary to decide if the B3LYP/6-311++G(d,p) or the G3B3 calculated barriers better reproduce the experimental observations.

In the TS structure, the electronic configuration of lone pair of the nitrogen adopts a configuration similar to that in a p orbital, being partially involved in the construction of multiple bonds with the atoms that surround it. Thus, a bond shortening is observed in the TS structures compared to those in the minimum.

The NBO analysis has shown the orbital interaction between the lone pair of the nitrogen and the π orbitals of the atoms attached to it as the main responsible of the small barrier found in those systems.

The electron density analysis has shown important differences in the characteristic of the CN bond in the minima and TS configurations.

Supplementary materials. – Coordinates of the optimized geometries at the B3LYP/6-311++G(d,p) computational level and imaginary frequency of the TS structures.

REFERENCES

1. a) E. L. Eliel and S. H. Wilen, *Stereochemistry of Organic Compounds*, John Wiley & Sons, Inc. New York, 1994, p. 550−555.
b) M. Oki, *Applications of Dynamic NMR Spectroscopy to Organic Chemistry*, VCH Publishers, Deerfield Beach, 1985.

2. J. M. Lehn, *Chem. Eur. J.* **12** (2006) 5910−5915.
3. F. Blanco, I. Alkorta, and J. Elguero, *J. Mol. Struct. (Theochem)* **847** (2007) 25−31.
4. A. D. Becke, *Phys. Rev. A* **38** (1988) 3098−3100.
5. A. D. Becke, *J. Chem. Phys.* **98** (1993) 5648−5652.
6. C. Lee, W. Yang, and R. G. Parr, *Phys. Rev. B* **37** (1988) 785−789.
7. P. A. Hariharan and J. A. Pople, *Theor. Chim. Acta* **28** (1973) 213−222.
8. M. J. Frisch, G. W. Trucks, H. B. Schlegel, G. E. Scuseria, M. A. Robb, J. R. Cheeseman, J. A. Montgomery, Jr., T. Vreven, K. N. Kudin, J. C. Burant, J. M. Millam, S. S. Iyengar, J. Tomasi, V. Barone, B. Mennucci, M. Cossi, G. Scalmani, N. Rega, G. A. Petersson, H. Nakatsuji, M. Hada, M. Ehara, K. Toyota, R. Fukuda, J. Hasegawa, M. Ishida, T. Nakajima, Y. Honda, O. Kitao, H. Nakai, M. Klene, X. Li, J. E. Knox, H. P. Hratchian, J. B. Cross, C. Adamo, J. Jaramillo, R. Gomperts, R. E. Stratmann, O. Yazyev, A. J. Austin, R. Cammi, C. Pomelli, J. W. Ochterski, P. Y. Ayala, K. Morokuma, G. A. Voth, P. Salvador, J. J. Dannenberg, V. G. Zakrzewski, S. Dapprich, A. D. Daniels, M. C. Strain, O. Farkas, D. K. Malick, A. D. Rabuck, K. Raghavachari, J. B. Foresman, J. V. Ortiz, Q. Cui, A. G. Baboul, S. Clifford, J. Cioslowski, B. B. Stefanov, G. Liu, A. Liashenko, P. Piskorz, I. Komaromi, R. L. Martin, D. J. Fox, T. Keith, M. A. Al-Laham, C. Y. Peng, A. Nanayakkara, M. Challacombe, P. M. W. Gill, B. Johnson, W. Chen, M. W. Wong, C. Gonzalez, and J. A. Pople, *Gaussian 03*, Gaussian, Inc., Pittsburgh PA, **2003**.
9. J. W. McIver and A. K. Komornicki, *J. Am. Chem. Soc.* **94** (1972) 2625−2633.
10. (a) L. A. Curtiss, K. Raghavachari, P. C. Redfern, V. Rassolov, and J. A. Pople, *J. Chem. Phys.* **109** (1998) 7764−7776; (b) A. G. Baboul, L. A. Curtiss, P. C. Redfern, and K. Raghavachari, *J. Chem. Phys.* **110** (1999) 7650−7657; (c) B. Anantharaman and C. F. Melius, *J. Phys. Chem. A* **109** (2005) 1734−1747.
11. A. E. Reed, L. A. Curtiss, and F. Weinhold, *Chem. Rev.* **88** (1988) 899.
12. R. F. W. Bader, *Atoms in Molecules: A Quantum Theory*, The International Series of Monographs of Chemistry; J. Halpen and M. L. H. Green (Eds.), Clarendon Press, Oxford, 1990.
13. F. W. Bieger-Konig, R. F. W. Bader, and T. H. Tang, *J. Comput. Chem.* **3** (1982) 317−328.
14. P. L. A. Popelier, with a contribution from R. G. A. Bone, MORPHY98, a topological analysis program, UMIST, Engl, EU, 1999.
15. O. Picazo and I. Alkorta, *Arkivoc* **ix** (2005) 305−320.
16. A. D. Becke and K. E. Edgecombe, *J. Chem. Phys.* **92 (**1990) 5397−5403.
17. S. Noury, X. Krokidis, F. Fuster, and B. Silvi, *Comput. Chem.* **23 (**1999) 597−604.
18. C. R. Kemnitz, G. B. Ellison, W. L. Karney, and W. T. Borden, *J. Am. Chem. Soc.* **122** (2000) 1098−1101
19. M. Kontoyianni, A. J. Hoffman, and J. P. Bowen, *J. Comput. Chem.* **13** (1992) 57−65.
20. J. M. Lehn and B. Munsch, *Theoret. Chim. Acta* **12** (1968) 91−94.
21. C. G. McCarty and D. M. Wieland, *Tetrahedron Lett.* **10** (1969) 1787−1790.
22. D. R. Armstrong and G. T. Walker, *J. Mol. Struct. (Theochem)* **149** (1987) 369−389.
23. Y. Shvo and A. Nahlieli, *Tetrahedron Lett.* **26** (1970) 4273−4274.
24. P. I. Nagy, J. Kokosi, A. Gergely, and A. Racz, *J. Phys. Chem. A* **107** (2003) 7861−7868.
25. A. Andrzejewska, L. Lapinski, I. Reva, and R. Fausto, *Phys. Chem. Chem. Phys.* **4** (2002) 3289−3296.
26. S. Nsikabaka, W. Harb, and M. F. Ruiz-López, *J. Mol. Struct. (Theochem)* **764** (2006) 161−166.
27. C. G. McCarty, in: S. Patai (Ed.), *The Chemistry of Carbon-Nitrogen Double Bond,* Chapter 9, Interscience, London, 1970, p. 401.
28. V. Bonačić-Koutecký and M. Persico, *J. Am. Chem. Soc.* **105** (1983) 3388−3395.
29. V. Bonačić-Koutecký and J. Michl, *Theor. Chim. Acta* **68** (1985) 45−55.
30. P. J. Bruna, V. Krumbach, and S. D. Peyerimhoff, *Can. J. Chem.* **63** (1985) 1594−1608.
31. R. Sumathi, *J. Mol. Struct. (Theochem)* **364** (1996) 97−106.
32. I. Frank, J. Hutter, D. Marx, and M. Parrinello, *J. Chem. Phys.* **108** (1998) 4060−4069.
33. N. L. Doltsinis and D. Marx, *Phys. Rev. Lett.* **88** (2002) 166402-1-16402-4.
34. I. Tavernelli, U. F. Roehrig, and U. Rothlisberger, *Mol. Phys.* **103** (2005) 963−981.
35. M. Oki, *Applications of Dynamic NMR Spectroscopy to Organic Chemistry*, VCH Publishers, Deerfield Beach, 1985. pp. 328, 336.
36. L. Pauling, in *The Nature of the Chemical Bond*, 2nd edition, Cornell University Press, Ithaca, 1945.
37. O. Knop, R. J. Boyd, and S. C. Choi, *J. Am. Chem. Soc.* **110** (1988) 7299−7301.
38. O. Knop, K. N. Rankin, and R. J. Boyd, *J. Phys. Chem. A.* **105** (2001) 6552−6566.
39. I. Alkorta, L. Barrios, I. Rozas, and J. Elguero, *Theochem* **496** (2000) 131−137.
40. E. Espinosa, I. Alkorta, J. Elguero, and E. Molins, *J. Chem. Phys.* **117** (2002) 5529−5542.
41. O. Picazo, I. Alkorta, and J. Elguero, *J. Org. Chem.* **68** (2003) 7485−7489
42. F. Blanco, D. H. O'Donovan, I. Alkorta, and J. Elguero, *Struct. Chem.* **19** (2008) 339−352.

SAŽETAK

Barijera oko dvostuke ugljik-dušik veze u iminskim derivatima (aldimini, oksimi, hidrazoni, azini)

Fernando Blanco, Ibon Alkorta i José Elguero

Instituto de Química Médica, C.S.I.C. Juan de la Cierva 3, E-28006 Madrid, Spain

Prikazani su rezultati istraživanja inverzijskog mehanizma imina i njihovih derivata (hidrazona, oksima, azina). Izračunate barijere [B3LYP/6-311++G(d,p) i G3B3 nivoi teorije] u dobrom su slaganju s malobrojnim eksperimentalnim podacima. Prijelazna stanja u svim slučajevima odgovaraju inverziji na dušiku osim u slučaju azina, gdje postoji nešto rotacijskog karaktera. Elektronska svojstva energetskih minimuma i prijelaznih stanja su okarakterizirana, što je omogućilo objašnjenje opaženih geometrijskih promjena tijekom procesa.